

Received January 19, 2022, accepted March 30, 2022, date of publication April 4, 2022, date of current version May 24, 2022.

Digital Object Identifier 10.1109/ACCESS.2022.3164522

# Ant Colony Optimization Tuned Closed-Loop Optimal Control Intended for Vehicle Active Suspension System

SAIBAL MANNA<sup>1</sup>, GEETHA MANI<sup>2</sup>, SUSHIL GHILDIYAL<sup>3</sup>,  
ALBERT ALEXANDER STONIER<sup>4</sup>, (Senior Member, IEEE),  
GENO PETER<sup>5</sup>, VIVEKANANDA GANJI<sup>6</sup>, AND SRINIVASAN MURUGESAN<sup>4</sup>

<sup>1</sup>Department of Electrical Engineering, NIT Jamshedpur, Adityapur, Jharkhand 831014, India

<sup>2</sup>School of Electrical Engineering, Vellore Institute of Technology, Vellore, Tamil Nadu 632014, India

<sup>3</sup>Department of Computer Science and Engineering, IIT Ropar, Rupnagar, Punjab 140001, India

<sup>4</sup>Department of Electrical and Electronics Engineering, Kongu Engineering College, Erode, Perundurai 638060, India

<sup>5</sup>CRISD, School of Electrical and Technology, University of Technology Sarawak, Sibu 96000, Malaysia

<sup>6</sup>Department of Electrical and Computer Engineering, Debre Tabor University, Debre Tabor 6300, Ethiopia

Corresponding author: Vivekananda Ganji (drvivek@bhu.edu.et)

**ABSTRACT** In recent years, the suspension system in modern vehicles has played a key role both as far as driving safety and comfort is concerned. To satisfy these vehicle performance specifications, active suspension is currently studied and implemented in practice in recent decades. In contrast to passive suspensions, by introducing force into system, active suspension can alter the suspension dynamic in real-time. A design of a controller is needed for real-time tuning of the control force in an active suspension system (ASS) to fulfill the challenging control objectives of suspension system comprising road handling, ride convenience, and travel suspension. This research proposed a novel ant colony optimization (ACO) algorithm for solving multi-objective weight optimization problem of the linear quadratic regulator (LQR) for automobiles ASS. The optimization problem of ASS is to design a state-feedback controller (SFC) as a result ACO is used to find optimal LQR weights. Here both Q and R weight matrix of LQR is tuned. On a quarter-car ASS (QCASS) system, the effectiveness of ACO-tuned LQR is analytically checked with hardware in loop (HIL) analysis for an irregular road surface. Here, for experiment, ISO road D rough runway, bumpy path, and pulse-type road profile are taken into account. Experimental findings illustrate that the proposed procedure can substantially reduce the acceleration of the Car body due to irregular road profiles compared to classical tuned LQR and model predictive control (MPC). The proposed controller shows the profound impact on the efficiency of the control schemes for three different road profiles.

**INDEX TERMS** ASS, ACO, bumpy road, ISO road D rough runway, LQR, MPC, periodic road, vehicle dynamics.

## I. INTRODUCTION

The suspension system, in automobiles, received significant attention in both academic and industry as it can enhance driving comfort, passenger safety, and road handling. Three types of suspension systems in the vehicle including active, semi-active, and passive suspensions, have been currently examined and implemented in practical use in recent decades to satisfy these performance criteria. ASS provides, improved

The associate editor coordinating the review of this manuscript and approving it for publication was Sudhakar Babu Thanikanti<sup>1</sup>.

control efficiency in contrast to passive suspension systems in terms of minimizing vehicle body movements attributed to road abnormalities. Several control strategies have been given for managing the ASS in the last three decades like adaptive control [1], [2],  $H_\infty$  [3], fuzzy, and sliding mode control [4], [5]. A genetic algorithm (GA) based optimization algorithm is introduced to tune the fuzzy membership function and PID parameter for QCASS. GA optimized FLC provides better control as compare to PID [6]. The challenging control aim of ASS, including suspension travel, body movement, and ride comfort, has driven researchers to implement

linear-quadratic control to optimize the most favorable performance without interruption. LQR, the basis of linear-quadratic Gaussian/loop transfer recovery (LQG/LTR) is an optimal SFC that provides dominance over robustness, assured stability, and a format that can be extended to MIMO systems. Since LQR provides a phase margin of  $(-600, 600)$  and gain margin of at least  $(-6, \infty)$  dB, several engineering applications were introduced, such as fuel cell technology [8], satellite attitude control [7], electric vehicles [9] to quad-rotors [10]. The correct choice of weighting matrices is the actual challenge for real-time application, instead of the effectiveness of LQR. No standard method for the optimal selection of LQR weight matrices is available. Though the initial choice of the penalty matrices is provided by Bryson's method, later on, it changes into a guess and check method, results in a time-consuming as well as tiring procedure. Therefore, less information regarding the influence of weighting matrices on the closed-loop presentation has inspired scientists to look into the efficiency of swarm intelligence techniques handling the LQR weight selection problem. A novel multi-objective archived based quantum particle optimizer (MOQPSO) is introduced and compared with the long-established COGA-II and NSGA-II algorithm on a half car and a bus suspension system [11].

A quantum behaved PSO (QPSO) is given by Hassani and Lee [12] to determine the LQR optimum design applied to two control problems named as the control of aircraft landing mechanism and the stabilization of the inverted pendulum. They introduced a combined dynamic weighting criterion, which dynamically incorporates the performance associate with the soft and hard constraints, and results are validated using a one-tailed T-test to see if the results are statistically relevant.

An adaptive inertia weight PSO is introduced to overcome the LQR multi-objective weight optimization problem for ASS [13]. For ASS, an MPC arrangement is given. A bench-scale clone of the QCASS for Quanser is being used to investigate the MPC scheme. The efficiency of the active suspension compared with that of an LQR control system and passive suspension to better understand the potential of the MPC [14]. Tsai et al., [15] applied PSO-based variable feedback gain control to resolve the automatic fighter tracking problems.

Simulation tests have shown that PSO-based LQR provided superior efficiency in vehicle tracking with minimum position error, relative to both linear matrix and Riccati equation (RE) based LQR approaches. The vision-based robot navigation [19], networked control system [18], unmanned air vehicle [17], smart structure control [20], and power quality conditioner [16] are some of PSO's noteworthy contributions to optimum controller design in the literature. One of the problems with conventional LQR is the selection of weighing matrices. Most of the researchers have tuned only one weighing matrices the remaining other matrices weights are fixed. But this problem can be resolved by the proposed algorithm. In the latest study, the vertical movement of QCASS

is considered. Here Both LQR weighing matrices are tuned with.

Therefore, this article has two main contributions:

1. The multi-objective suspension control of QCASS is formulated as an optimization problem and SFC gains are optimized using the ACO tuned LQR that improves the convergence speed.
2. The effectiveness of the formulated scheme to improve ride comfort while maintaining passenger safety is experimentally evaluated on lab level ASS. The efficiency of the proposed scheme is validated experimentally on a QCASS for three different road surfaces such as bumpy road, ISO road D rough runway, and pulse profile.

A novel ACO is proposed to tune the two weighing matrices (R and Q) of LQR. Further paper is structured as follows. Section II represents performance measures and dynamics of ASS. Section III describes the problem formulation for the optimal LQR design. Section IV presents the real ant description, mathematical model, and optimal weight of the ACO algorithm. Section V provides the Experimental validation and statistical analysis of ACO tuned LQR, Classical tuned LQR and MPC under three different road surfaces. Section VI gives the concluding remark of the paper.

## II. ACTIVE SUSPENSION SYSTEM

### A. SYSTEM DYNAMICS

The vertical dynamics of a QCASS block diagram are presented in Fig.1, consisting of two mass-spring-damper

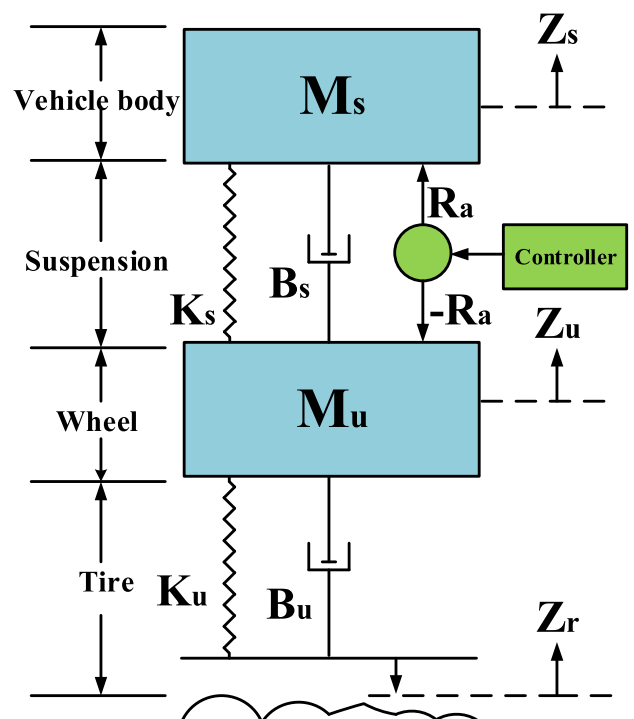


FIGURE 1. Block diagram of the QCASS.

systems. This system is a product of an unsprung ( $M_u$ ) and a sprung mass ( $M_s$ ), which signify the wheel mounting and the car body in the QCM. Both  $M_u$  and  $M_s$  are sustained by dampers and springs. The bottom damper and spring represent the damping factor ( $B_u$ ) and tire stiffness coefficient ( $K_u$ ) to the road. Similarly, the bodyweight over the tire is balanced by a damper ( $B_s$ ) and spring ( $K_s$ ).  $Z_u$  and  $Z_s$  represent the  $M_u$  and  $M_s$  vertical displacement respectively.  $Z_r$  indicates vertical road displacement due to external force. The system includes an electrical actuator located between the wheel assembly and car body to counteract the vertical forces ( $R_a$ ) generated by an irregular ground surface. The mathematical equation of the ASS is formulated by using the Newton laws of motion. The equations are given below,

For  $M_u$ ,

$$M_u \ddot{Z}_u = -B_u \dot{Z}_u - B_s \dot{Z}_u + B_u \dot{Z}_r - R_a - (Z_u - Z_s)K_u - (Z_u - Z_s)K_s \quad (1)$$

For  $M_s$

$$M_s \ddot{Z}_s = R_a + B_s \dot{Z}_u - B_s \dot{Z}_s - (Z_s - Z_u)K_s \quad (2)$$

The following state and input vectors are considered for achieving the system state-space model,

$$x = \left[ Z_s - Z_u \quad \dot{Z}_s \quad Z_u - Z_r \quad \dot{Z}_u \right]^T \quad \text{and} \quad u_i = R_a$$

The system state-space model is obtained below

$$\begin{aligned} \dot{x}(t) &= \begin{bmatrix} 0 & 1 & 0 & 1 \\ -\frac{K_s}{M_s} & -\frac{B_s}{M_s} & 0 & \frac{B_s}{M_s} \\ 0 & 0 & 1 & 0 \\ \frac{K_s}{M_u} & \frac{B_s}{M_u} & -\frac{K_u}{M_u} & -\frac{B_s + B_u}{M_u} \end{bmatrix} z(t) \\ &+ \begin{bmatrix} 0 \\ \frac{1}{M_s} \\ 0 \\ -\frac{1}{M_u} \end{bmatrix} u_i(t) \\ y(t) &= \begin{bmatrix} 1 & 0 & 0 & 0 \\ -\frac{K_s}{M_s} & -\frac{B_s}{M_s} & 0 & \frac{B_s}{M_s} \end{bmatrix} z(t) + \begin{bmatrix} 0 \\ -\frac{1}{M_s} \end{bmatrix} u_i(t) \end{aligned} \quad (3)$$

where  $\dot{Z}_s$  and  $\dot{Z}_u$  are the vertical velocity of the car body and tire respectively.  $Z_u - Z_r$  and  $Z_s - Z_u$  are the vertical tire deflection and suspension deflection respectively. The control force ( $R_a$ ) acts as a control input ( $u_i(t)$ ), generated by an electrical actuator. The outputs are vertical suspension

deflection and vertical car acceleration ( $\ddot{Z}_s$ ). The ASS parameter specification is listed in Table 1.

TABLE 1. ASS parameters [13].

Parameter	Value
$M_s$	2.45 kg
$M_u$	1 kg
$B_s$	7.5 N-s <sup>2</sup> /m
$B_u$	5 N-s <sup>2</sup> /m
$K_s$	490 N/m
$K_u$	1020 N/m
Accelerometer sensitivity	9.81 m/s <sup>2</sup> /V
Suspension travel range	0.038 m
Suspension motor torque constant	112×10 <sup>-3</sup> N-m/A
Suspension encoder resolution	0.000942m/count

### B. PERFORMANCE MEASURES

The following requirement must be taken into account while designing a feedback controller for ASS:

- Ride comfort: The aim is to increase passengers comfort in the car suspension system by decreasing the  $\ddot{Z}_s$  from a rough road surface.
- Suspension travel: The ASS must guarantee that the suspension deflection is regulated in the acceptable range while maintaining a minimum body acceleration, avoiding any structural damage:

$$|Z_s - Z_u| \leq Z_{max} \quad (4)$$

- Road handling: It is at the utmost importance that the wheel assembly maintains firm road contact to ensure the traveller's safety. Thus, the static load of the tire must be stronger than the dynamic load:

$$|K_s(Z_u - Z_r)| \leq (M_s + M_u)g \quad (5)$$

Table 2 shows the maximum value of each state variable [21]. We intend to synthesize an optimized SFC based on linear quadratic theory to realize a feedback controller capable of overcoming these competing control objectives.

TABLE 2. Maximum value of state variables [21].

State Variables	Maximum Value
Vertical suspension deflection	0.038 m
Vehicle body vertical velocity	2.45 m/s
Vertical tire deflection	0.038 m
Tires vertical velocity	2.45 m/s

### III. PROBLEM FORMULATION

The linear-quadratic optimal control problem for the LTI system is as follows:

Consider the system

$$\begin{aligned} \dot{x}(t) &= Ex(t) + Fu_i(t), t \geq 0, x(0) = x_0 \\ y(t) &= Gx(t) + Hu_i(t), t \geq 0 \end{aligned} \quad (6)$$

The optimal control input  $u_i^*(t)$  is to be found, with this initial condition  $x(0) = x_0$ , so that  $u_i^*(t)$  can regulate the system dynamics to the desired state by evaluating the below objective function:

$$J(u_i^*) = \int_0^\infty x^T(t)Qx(t) + u_i^T(t)Ru_i(t)dt \quad (7)$$

where  $R = R^T$  and  $Q = Q^T$  are the positive definite and positive semi-definite state weighing matrix respectively. The LQR weighing matrices are chosen to be diagonal matrices to make the cost function quadratic. The number of control input and number of state decides the order of  $R$  and  $Q$  matrix. If  $(E, F)$  pair and  $(E, G)$  pair proves to be controllable and observable respectively, then LQR applies in the following optimal state feedback law:

$$u_i = -Lx(t) \quad (8)$$

where  $L$  is the optimal SFC gain obtained from the Lagrange optimization approach:

$$L = R^{-1}F^T T \quad (9)$$

By solutions of the following RE, a transformation matrix  $T$  can be achieved:

$$E^T T + TE + Q - TFR^{-1}F^T T = 0 \quad (10)$$

However, the problem with LQR is the selected technology of weighing matrices, due to the lack of understanding of the connections between closed-loop output and quadratic weights. To fix the LQR weights optimization problem, an ACO algorithm is introduced.

#### IV. ANT COLONY OPTIMIZATION ALGORITHM

At first, Dorigo introduced ACO algorithms [22]–[24].

##### A. REAL ANTS DESCRIPTION

This algorithm is related to that of real ants behavior belongs to the social insect family. A community of ants, however, leaves their colony in order to find out the source of food in a random direction and imprints their path by putting a chemical material on the surface. The path has the highest amount of pheromones, which decays over time, and attracts other ants. A shorter route with a higher number of pheromones than a longer route is then found. So, through indirect communication medium called pheromones, which are set on the ground as a reference for other ants, the shortest path can be identified between food and nest. The shortest route between food and nest can be found for real ants in Fig. 2. [25]. There are no barriers between food source and nest as displayed in Fig. 2a. However, the path is straight. If there is a barrier in between ants path, few ants pick the left side across the barrier and

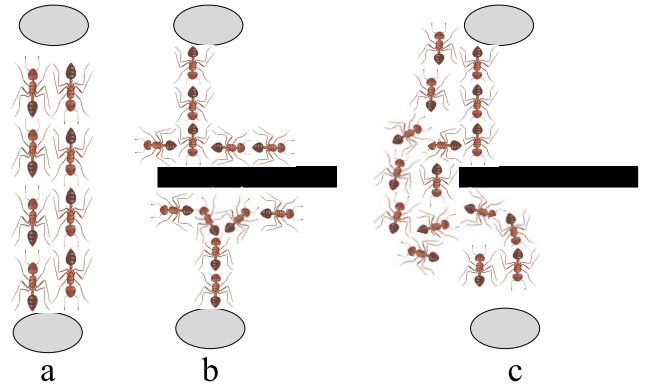


FIGURE 2. Real ant behaviour [25].

the other chooses the right side, as seen in the Fig. 2b; the pheromone put to the left is concentrated than to the right of the barrier as the ants need a minimum time in the shortest way to leave and go back to the nest at the same speed. So, they placed a greater quantity of pheromones on the other path than other ants, while the other ants are attracted to the shortest path. Therefore, as seen in Fig.2c, all colony ants choose the shortest path across the barrier.

##### B. MATHEMATICAL MODEL

After each ant completed its journey, an arbitrary amount of pheromone is placed in each path as a result other ants are attracted to the shortest path by the probabilistic transition rule (PTR), which relies on the amount of pheromone deposition and a heuristic guide function (HGF) equal to the inverse of the distance between initial and final of the path. The PTR of ant  $a$  to go from location  $m$  to location  $n$  can be described as in Traveling Salesman Problem (TSP) [24] as:

$$P_{ij}^k(t) = \frac{[\mu_{mn}(t)]^\gamma [\varphi_{mn}(t)]^\lambda}{\sum_q [\mu_{mq}(t)]^\gamma [\varphi_{mn}(t)]^\lambda}, \quad n, q \in N_m^k \quad (11)$$

where,  $\mu_{mn}$  is the pheromone deposited by ant  $a$  between location  $m$  and  $n$ ,  $\varphi_{mn}$  is the visibility and equal to the inverse of transition cost or distance between location  $m$  and  $n$  ( $\varphi_{mn} = 1/d_{mn}$ ).  $\gamma$  is pheromone trail relative weight and  $\lambda$  is the HGF. If  $\gamma = 0$ , the nearest location selected similar to a classical greedy algorithm. On the other hand, if  $\lambda = 0$ , the probability will be depending only on  $\gamma$ . The  $\gamma$  and  $\lambda$  should be tuned together, the best value of  $\lambda$  and  $\gamma$  are 5 and 1 respectively, founded experimentally by Dorigo [24];  $q$  is the location to be visited after city  $m$  whereas  $N_m^k$  is a tabu list in ant's memory that recodes the cities to visit so as to avoid stagnations. A local pheromone update is calculated by each ant after each tour is finished, based on the path of each ant, as in Eq. (12); after all, ants have opted the shortest path, a global pheromone update would objectify the impact of the latest additional ants deposit that draw into the best tour as seen in Eq. (13):

$$\mu_{mn}(t + 1) = (1 - \rho)\mu_{mn}(t) + \rho\mu_0 \quad (12)$$

$$\mu_{mn}(t + 1) = (1 - \rho)\mu_{mn}(t) + \varepsilon\Delta\mu_{mn}(t) \quad (13)$$

where  $\mu_{mn}(t+1)$  is pheromone after one iteration or tour,  $\rho$  and  $\varepsilon$  is the pheromone evaporation constant and elite path weighting constant,  $\mu_o = 1/d_{mn}$  is the incremental value of pheromone of each ant.  $\Delta\mu_{mn}$  is pheromone amount for elite path as:

$$\Delta\mu_{ij}(t) = \frac{1}{d_{best}} \quad (14)$$

where  $d_{best}$  is the shortest tour distance.

### C. ACO ALGORITHM FOR THE WEIGHT PROBLEM

This algorithm in this article is used as a method of optimization to overcome the LQR weight problem with dependent and control variable constraints in which artificial ants are looking for the shortest path that contains a minimum objective function and the strongest pheromone trail. Our goal in this article is to minimize the  $\ddot{Z}_s, Z_s - Z_u$  and assembly of the wheel, to ensure firm road contact.

A search space in the ACO algorithm develops with dimensions of stages on many states and control variables or randomly distributed control variables values within a reasonable threshold. Artificial ants leave the colony to look arbitrarily in the search space based on the probability in (11) of completing a tour matrix composed of ant locations of the same search space dimension. The tour matrix is then introduced on the objective function of finding an HGF to reach the best solution and update global and local pheromone to start the next iteration. System parameters are tuned to find the optimal value of these parameters through trial and error. To solve the LQR weight problem, the ACO is used. The flowchart of ACO is displayed in Fig. 3.

The multi-objective suspension control based on novel ACO-tuned LQR is shown in Fig.4. The tire displacement and suspension travel are calculated using optical encoders, differentiator, and a second-order low pass filter ( $\omega_n = 15.7$  rad/sec) is used to obtain tire and suspension velocity.

$$H(s) = \frac{\omega_n^2}{s^2 + 2\xi\omega_n s + \omega_n^2} \quad (15)$$

The Q matrix is a  $4 \times 4$  matrix because ASS is a 4<sup>th</sup> order model. Hence, the obtained cost function to be optimized is

$$J = \int_0^\infty (q_1x_1^2 + q_2x_2^2 + q_3x_3^2 + q_4x_4^2 + R_1u_1^2)dt \quad (16)$$

where  $q_1$  and  $q_2$  are the suspension travel and suspension velocity weight.  $q_3$  and  $q_4$  are the weights of tire deflection and tire velocity. Likewise,  $R_1$  is the control force weight factor. To optimize LQR weight the following integral absolute error (IAE) is known as the fitness function:

$$IAE = \int_0^\infty |e|dt \quad (17)$$

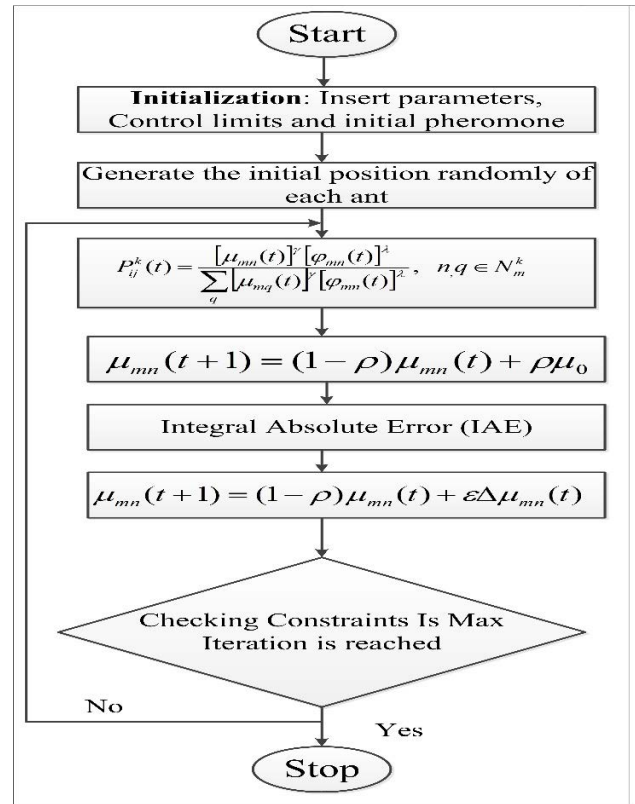


FIGURE 3. ACO algorithm flow chart.

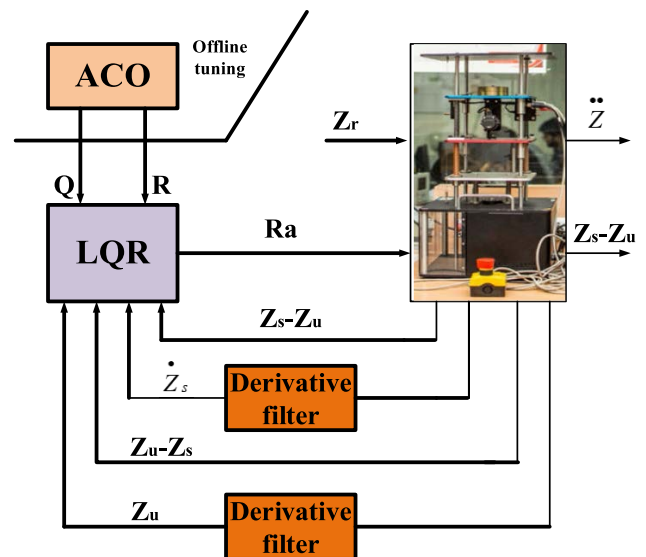


FIGURE 4. Proposed ACO-tuned LQR for QCASS [12].

The goal is to find the LQR optimum weights and evaluate the state feedback gain vector  $L = [l_1, l_2, l_3, l_4]$  such that the controller can achieve the ASS objectives.

### V. EXPERIMENTAL RESULTS AND DISCUSSION

The entire experiment is performed on the laboratory-based ASS as shown in Fig.5. ASS workstation consisting of

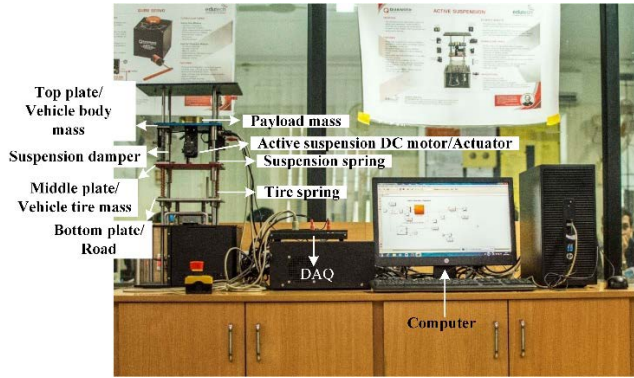


FIGURE 5. Quarter Car ASS workstation [1].

TABLE 3. Weighting and feedback gain matrices of LQR.

Controller	Weighting matrices	Feedback Gain matrix
Classical tuned LQR	$Q = \text{diag}(692.52, 0.16, 692.52, 0.16)$ $R = 6.50e-04$	$[469.4581$ $45.8711$ $-91.5474$ $-12.8517]^T$
ACO tuned LQR	$Q = \text{diag}(246.0576, 176.9057, 86.9232, 8.6696)$ $R = 0.0037$	$[36.6504632397722$ $217.276049371267$ $1030.73836445864$ $-12.9216285336431]^T$

three vertical plates on top of each other is shown in Fig.5. The top plate hanging over the central plate with two springs mimics the car body and provides an accelerometer to obtain car body acceleration to the plant surface. To overcome the vertical forces produced by an irregular road, a servomotor inserted between central and top plates serves as an actuator. The central plate, via a spring, establishes a connection with the lower plate. The plate at the bottom that similar to the quarter car wheel is attached to the DC motor to create systems road exciting. The motor torque-based circular motion is converted into linear motion using the lead gear and screw system to create various road patterns.

The ASS experimental setup comprises a QCASS workspace interfacing with a PC, a USB-based 8 channel data acquisition module (DAQ), and power amplifiers. It comprises three optical encoders with a resolution of 4096 counts/revolution in quadrature mode for the measurement of tire displacement and suspension deflection. The upper plate is also connected with an accelerometer ( $\pm 10g$  range) to achieve car body acceleration relative to the surface. A controlled supply of  $\pm 10V$  at 3A can be offered by the power amplifiers which drive the servomotors. The received sample rate of the DAQ board, which has a 12bit resolution, is 500 Hz. Using the Quanser real-time control prototype software, the control algorithm implemented in simulink is linked to the ASS workstation for HIL research.

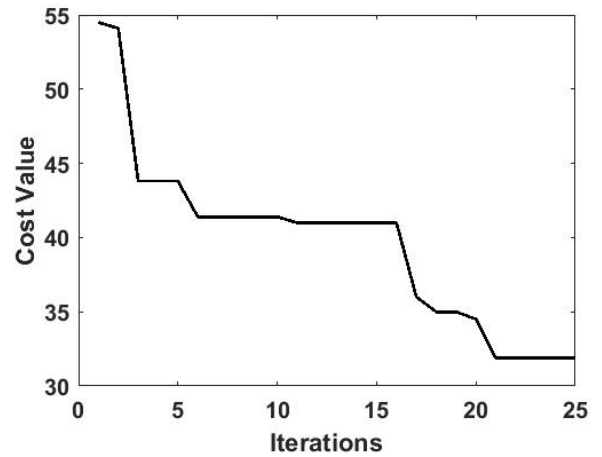


FIGURE 6. Fitness function plot.

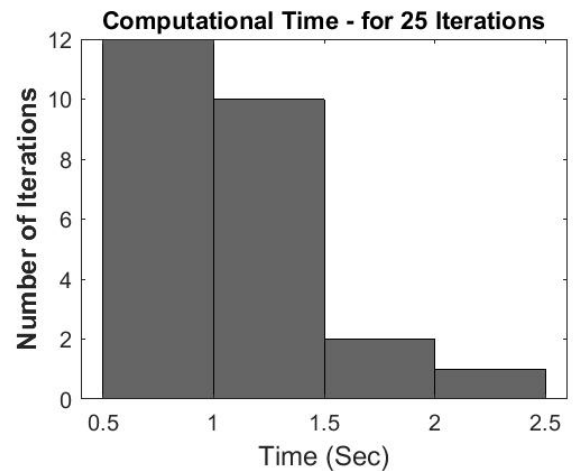


FIGURE 7. Histogram for the computational complexity of ACO iteration.

The tuning expression of the Q matrix and R matrix for classical tuned LQR is given (18).

$$Q_{ii} = \frac{1}{(\text{Maximum of each state})^2}$$

$$R_{ii} = \frac{1}{(\text{Maximum of the } R_a)^2} \quad (18)$$

Four ACO parameters need to be chosen: ant population (a), a parameter for controlling the relative importance of pheromone ( $\gamma$ ), a parameter for controlling the relative importance of local heuristic factor ( $\lambda$ ), and the pheromone coefficient ( $\rho$ ). To achieve good results, we must choose the proper range of  $\gamma$  and  $\lambda$ , generally,  $\gamma = 0.5$  to  $5$ ,  $\lambda = 0$  to  $5$  [26]. We developed an offline ACO tuning strategy using the simulation comprised of a suspension system model and the ACO technique successfully finds the global optimum solution in the simulation settings through different combinations of parameters. Optimal ranges for these ACO parameters are suggested as an outcome of the investigation ( $\gamma = 0.6$  to  $0.9$ ,  $\lambda = 0.2$  to  $0.5$ , ant population (a) =  $100$  to  $200$ ,  $\rho = 0.88$ ). The maximum number of iterations

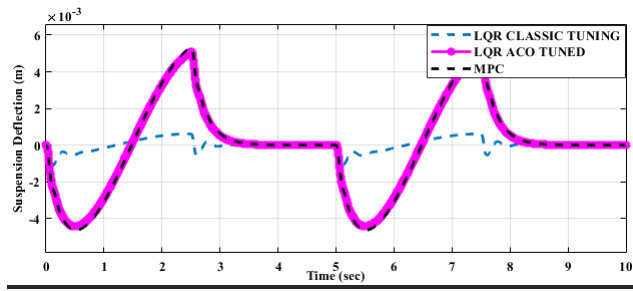


FIGURE 8. Suspension deflection of three controllers under bumpy road profile.

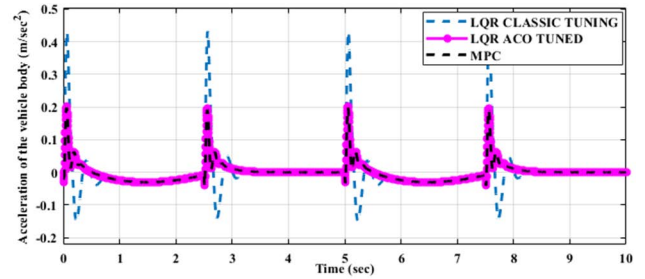
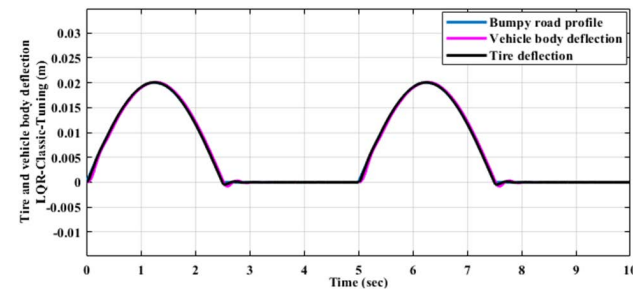
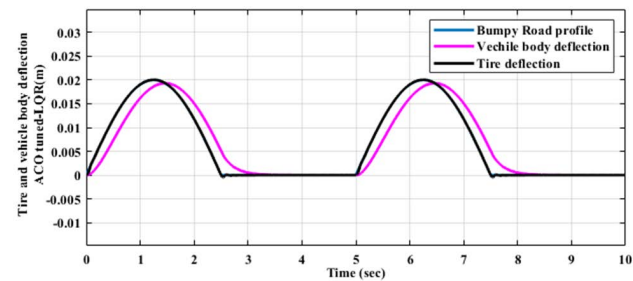


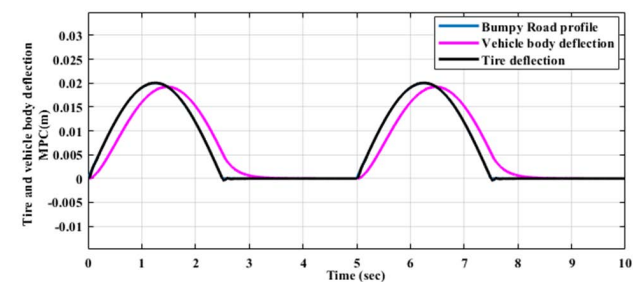
FIGURE 10. Vehicle body acceleration of three controllers under bumpy road profile.



(a)



(b)



(c)

FIGURE 9. Tire and Vehicle body deflection for (a) Classical-LQR (b) ACO-LQR (c) MPC under bumpy road profile.

is 25. Fig. 6 shows the convergence of the fitness function for ACO. Fig. 7 shows the Histogram for the computational complexity of ACO iteration. From the histogram, it has been observed that computational time is less for obtaining an optimal solution even for more number of iterations due to colony Intelligence. Table 3 gives the optimized input weight matrices and feedback gain matrix of classical tuned and ACO tuned LQR.

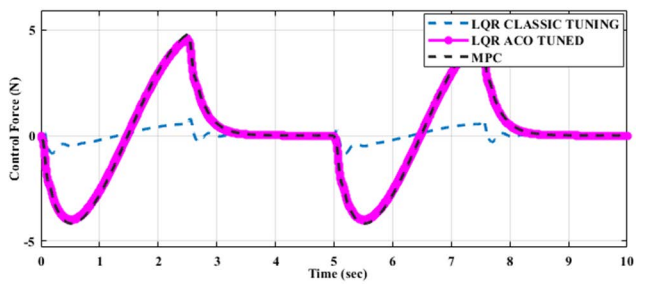


FIGURE 11. Control force of three controllers under bumpy road profile.

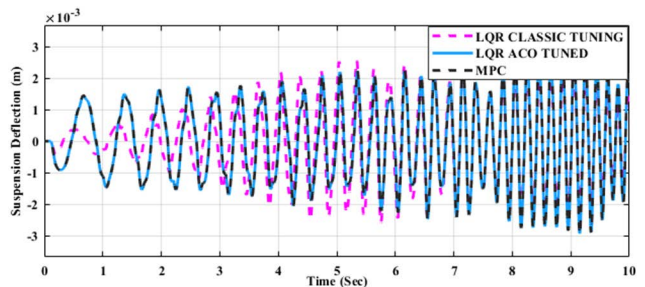


FIGURE 12. Suspension deflection of three controllers under ISO road D rough road profile.

In case of MPC controller, the parameters are: sampling time 0.1 sec, Prediction horizon = 15, control horizon = 3, Output Error weighting Matrix  $WE/(Q \text{ in MPC}) = [100 \ 0; 0 \ 10]$ ; and Control action Weighing matrix  $Wu/(R \text{ in MPC}) = [10]$ .

The performance of the Controller is checked for three different road input types: a bumpy, an ISO road D rough runway, and a pulse road profile.

*Case 1 (Bumpy Road Profile):* The amplitude of the bumpy road profile is considered as 0.02m [13]. Fig. 8 showing the suspension deflection response of classical tuned LQR, ACO tuned LQR and MPC reveals that ACO tuned LQR results in better steady-state response and regulates the suspension movement near road profile to prevent tire damage. Fig. 9 indicate the deflection of the tire, shows that the vertical displacement of the tire is accurately controlled to follow the road profile in ACO tuned LQR relative to others controller to ensure the safety of travelers. Also, the vertical

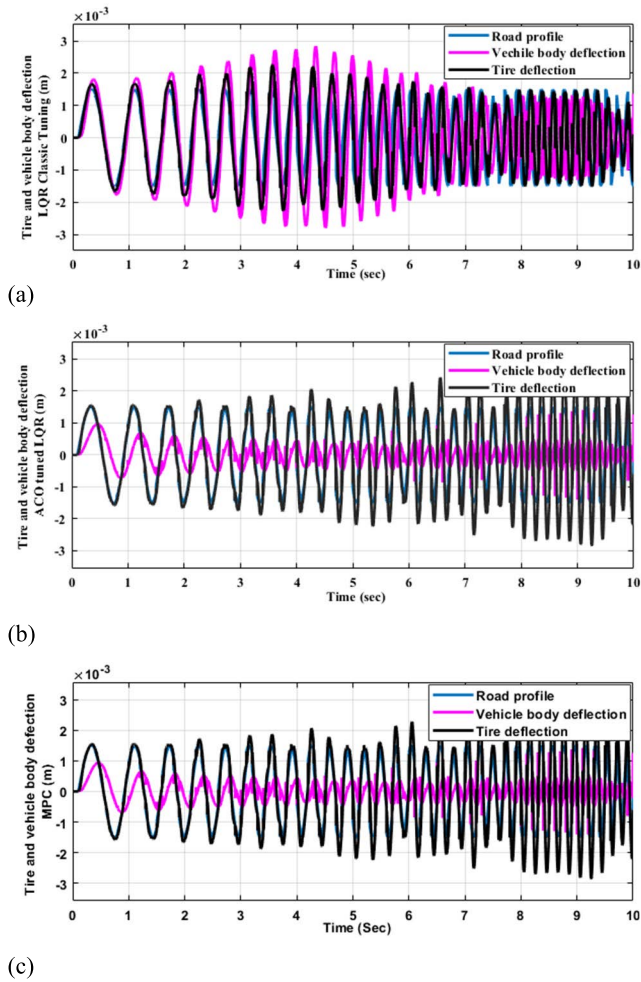


FIGURE 13. Tire and Vehicle body deflection for (a) Classical-LQR (b) ACO-LQR (c) MPC under ISO road D rough runway profile.

vehicle body acceleration in Fig. 10 seems to test passengers traveling comfort. Car acceleration is low in ACO tuned LQR compared to other controllers. ACO-tuned LQR provides better results compared to other controllers. Fig. 11 shows that the force is limited within  $\pm 5$  N for possible control input. The above discussion and figure show that all the state variable constraints are within the maximum value or near the maximum value as given in table 2.

*Case II (ISO Road D Rough runway):* The maximum amplitude of an ISO Road D Rough runway profile is considered as 0.015m and run at 90 km/h [27]. Fig. 12 shows the vertical suspension deflection for three controllers. Fig. 13 shows the tire and vehicle body deflection for three controllers. Fig. 14 shows the vertical vehicle body acceleration of the three controllers. Car acceleration is low in ACO tuned LQR compared to other controllers. In this road profile, the ACO-tuned LQR provides better results compared to other controllers. Fig. 15 shows that the force is limited within  $\pm 3$  N for possible control input. The above discussion and figure show that all the state variable constraints are within the maximum value or near the maximum value as given in Table 2.

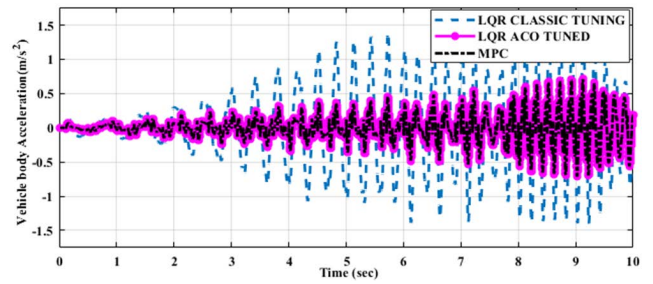


FIGURE 14. Vehicle body acceleration of three controllers under ISO road D rough runway.

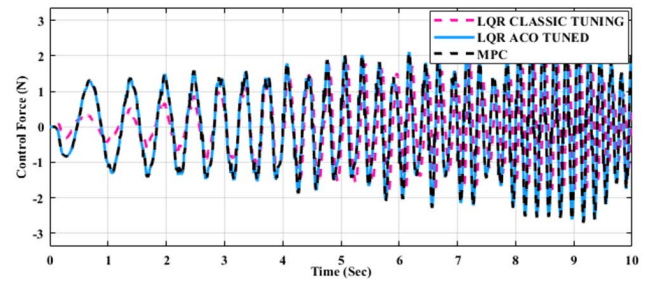


FIGURE 15. Control force of three controllers under ISO road D rough runway.

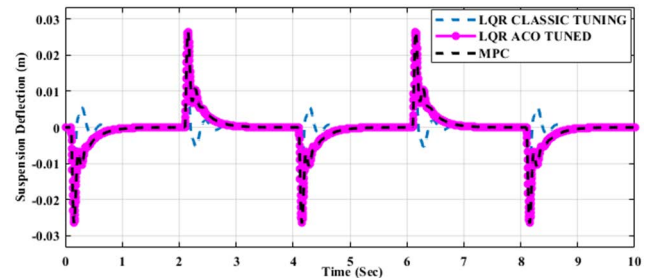
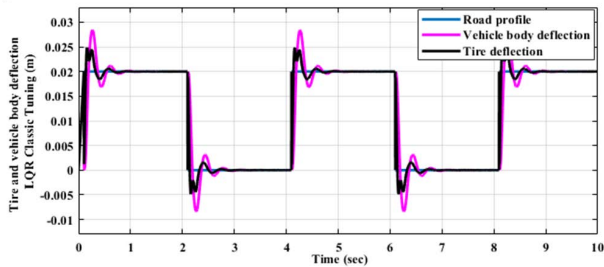


FIGURE 16. Suspension deflection of three controllers under pulse road profile.

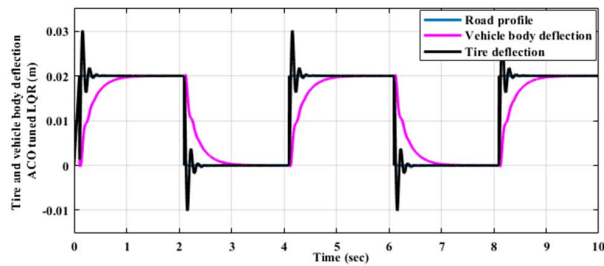
*Case III (Periodic/Pulse Road Profile):* The amplitude of pulse/periodic road profile is considered as 0.02m [13]. Fig. 16 shows the vertical suspension deflection for three controllers. Fig. 17 shows the vertical tire and vehicle body deflection for three controllers. Fig. 18 shows the vertical vehicle body acceleration of the three controllers. Car acceleration is low in ACO tuned LQR compared to other controllers. In this road profile, the ACO -tuned LQR provides better results compare to other controllers. Fig. 19 shows that the force is limited within  $\pm 25$  N for possible control input. The above discussion and figures show that all the state variable constraints are within the maximum value or near the maximum value as given in Table 2.

The proposed algorithm outperforms the classical-tuned LQR as well as MPC and significantly improves ride comfort. The performance matrices considered here is root means square (RMS) of vertical suspension travel, which is

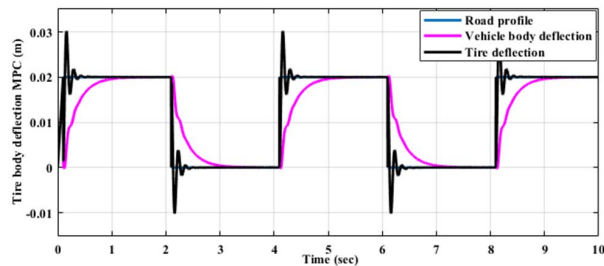




(a)



(b)



(c)

**FIGURE 17. Tire and Vehicle body deflection for (a) Classical-LQR (b) ACO-LQR (c) MPC under pulse road profile.**

mathematically described below:

$$\text{RMS suspension travel} = \left\{ \frac{1}{T} \int_0^T [Z_s(t) - Z_u(t)]^2 dt \right\}^{\frac{1}{2}} \quad (19)$$

The performance metrics for three road profiles under various controllers are given in Table 4. The RMS value of ACO-tuned LQR and MPC gives a lower value compared to PSO-tuned LQR [13] and AIWPSO tuned LQR [13] controller under bumpy road profile. For three road profile, compare to classical tuned LQR, the ACO tuned LQR and MPC gives a better result. The proposed controller gives a minimum RMS value compares to other controllers. Minimum RMS value means low vibration. So, the road handling capacity and ride comfort of the passenger is improved by using the proposed controller. RMS value of MPC and proposed controller gives almost the same value under three road profiles. But MPC takes more computational time to compare with ACO tuned LQR. Table 5 shows the runtime comparison of ACO tuned LQR and MPC controller under three road profiles. If any mismatch occurs the MPC cannot work systematically but the ACO tunes LQR works systematically.

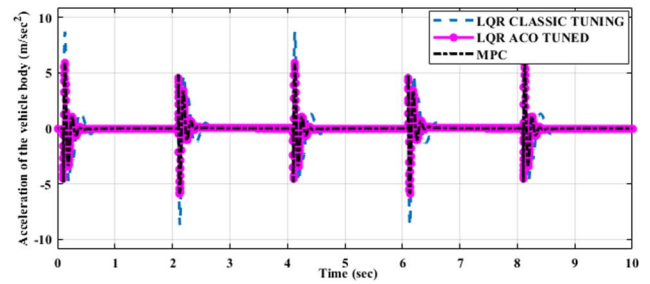


**FIGURE 18. Vehicle body acceleration of three controllers under pulse road profile.**

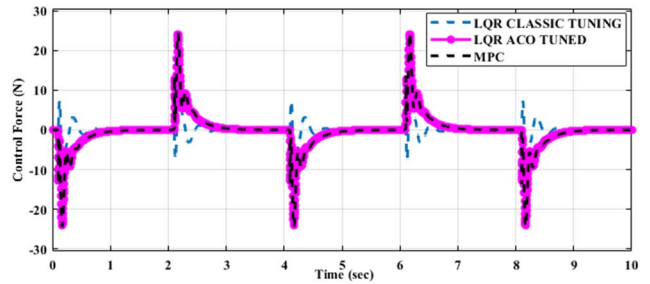


**FIGURE 19. Control force of three controllers under pulse road profile.**

**TABLE 4. Performance indices for ASS.**

Road Profile	Controller	RMS(m/s <sup>2</sup> )
Bumpy Road	Classical tuned LQR	0.0730
	ACO tuned LQR	0.0323
	MPC	0.0316
	PSO tuned LQR [13]	0.413
	AIWPSO tuned LQR [13]	0.291
ISO road D rough runway	Classical tuned LQR	0.6277
	ACO tuned LQR	0.2271
	MPC	0.2238
Pulse/ Periodic Road	Classical tuned LQR	1.4325
	ACO tuned LQR	0.9062
	MPC	0.9195

**TABLE 5. Run time comparison.**

Road Profile	ACO tuned LQR	MPC
Clock precision: 0.0000005 sec		
Clock Speed: 2201MHz		
Bumpy Road	19.45 sec	21.56 sec
ISO road D rough runway	26.19 sec	28.61 sec
Pulse/ Periodic Road	18.80 sec	22.42 sec

These metrics emphasize that, by ensuring firm contact of the tire with the road surface, the proposed system enhances not only traveler comfort but also safety considerably.

## VI. CONCLUSION

This paper introduces a novel ACO tuned LQR method of solving the LQR weight optimization problem applied to laboratory-based vehicle suspension systems. The problem of selection of the LQR weight is formulated as an Optimization problem and the ACO is used to find the best

weights. Both the weight matrices of LQR are tuned using this proposed algorithm. In terms of ride comfort, suspension travel, and road handling capability, the control scheme offers better performance compared to Classical-LQR and MPC controller. Three separate road profiles confirmed this efficiency outcome. The performance indices highlight that better results are provided by the proposed controller. While MPC and the algorithms proposed to give nearly the same result but MPC takes more runtime than ACO tuned LQR. On a QCASS for realistic road profiles, the effectiveness of the proposed system is experimentally verified. The experimental findings confirm that the proposed scheme greatly increases the road handling and comfort of passengers. A camera-based ASS can provide significantly improved performance results. The camera is used to recognize the state of route or road (Bumpy, periodic, etc.); standard sensors are used to measure angular velocity. The camera data are compared and verified in synchronization with the processing of the camera image. The suspension control can be enhanced more accurately with this.

## REFERENCES

- [1] S. Manna and R. Mazumdar, "Comparative performance analysis of LQR and MPC for active suspension system," in *Proc. IEEE 5th Int. Conf. Comput. Commun. Autom. (ICCCA)*, Greater Noida, India, Oct. 2020, pp. 352–356, doi: [10.1109/ICCCA49541.2020.9250813](https://doi.org/10.1109/ICCCA49541.2020.9250813).
- [2] I. Fialho and G. J. Balas, "Road adaptive active suspension design using linear parameter-varying gain-scheduling," *IEEE Trans. Control Syst. Technol.*, vol. 10, no. 1, pp. 43–54, Jan. 2002.
- [3] X. Shao, F. Naghdy, and H. Du, "Reliable fuzzy  $H_\infty$  control for active suspension of in-wheel motor driven electric vehicles with dynamic damping," *Mech. Syst. Signal Process.*, vol. 87, pp. 365–383, Mar. 2017.
- [4] V. S. Deshpande, B. Mohan, and P. D. Shendge, "Disturbance observer based sliding mode control of active suspension systems," *J. Sound Vib.*, vol. 333, no. 11, pp. 2281–2296, May 2014.
- [5] J. Lin, R.-J. Lian, C.-N. Huang, and W.-T. Sie, "Enhanced fuzzy sliding mode controller for active suspension systems," *Mechatronics*, vol. 19, no. 7, pp. 1178–1190, Oct. 2009.
- [6] M. P. Nagarkar, Y. J. Bhalerao, G. J. V. Patil, and R. N. Z. Patil, "GA-based multi-objective optimization of active nonlinear quarter car suspension system—PID and fuzzy logic control," *Int. J. Mech. Mater. Eng.*, vol. 13, p. 10, Nov. 2018, doi: [10.1186/s40712-018-0096-8](https://doi.org/10.1186/s40712-018-0096-8).
- [7] J. Cao, P. Li, and H. Liu, "An interval fuzzy controller for vehicle active suspension systems," *IEEE Trans. Intell. Transp. Syst.*, vol. 11, no. 4, pp. 885–895, Dec. 2010.
- [8] H. Arefkhani, S. H. Sadati, and M. Shahravi, "Satellite attitude control using a novel constrained magnetic linear quadratic regulator," *Control Eng. Pract.*, vol. 101, Aug. 2020, Art. no. 104466.
- [9] M. Habib, F. Khoucha, and A. Harrag, "GA-based robust LQR controller for interleaved boost DC–DC converter improving fuel cell voltage regulation," *Electr. Power Syst. Res.*, vol. 152, pp. 438–456, Nov. 2017.
- [10] Z. Han, N. Xu, H. Chen, Y. Huang, and B. Zhao, "Energy-efficient control of electric vehicles based on linear quadratic regulator and phase plane analysis," *Appl. Energy*, vol. 213, pp. 639–657, Mar. 2018.
- [11] E. Grotti, D. M. Mizushima, A. D. Backes, M. D. de Freitas Awruch, and H. M. Gomes, "A novel multi-objective quantum particle swarm algorithm for suspension optimization," *Comput. Appl. Math.*, vol. 39, p. 105, Mar. 2020, doi: [10.1007/s40314-020-1131-y](https://doi.org/10.1007/s40314-020-1131-y).
- [12] K. Hassani and W.-S. Lee, "Multi-objective design of state feedback controllers using reinforced quantum-behaved particle swarm optimization," *Appl. Soft Comput.*, vol. 41, pp. 66–76, Apr. 2016.
- [13] J. S. David Reddipogu and V. K. Elumalai, "Hardware in the loop testing of adaptive inertia weight PSO-tuned LQR applied to vehicle suspension control," *J. Control Sci. Eng.*, vol. 2020, Oct. 2020, 8873995, doi: [10.1155/2020/8873995](https://doi.org/10.1155/2020/8873995).
- [14] R. R. Das and V. Kumar, "Active suspension with model predictive control," *Int. J. Eng. Adv. Technol.*, vol. 8, no. 6, pp. 2826–2831, Aug. 2019, doi: [10.35940/ijeat.F9038.088619](https://doi.org/10.35940/ijeat.F9038.088619).
- [15] S.-J. Tsai, C.-L. Huo, Y.-K. Yang, and T.-Y. Sun, "Variable feedback gain control design based on particle swarm optimizer for automatic fighter tracking problems," *Appl. Soft Comput.*, vol. 13, no. 1, pp. 58–75, Jan. 2013.
- [16] S. B. Karanki, M. K. Mishra, and B. K. Kumar, "Particle swarm optimization-based feedback controller for unified power-quality conditioner," *IEEE Trans. Power Del.*, vol. 25, no. 4, pp. 2814–2824, Oct. 2010.
- [17] H. B. Duan and S. Q. Liu, "Non-linear dual-mode receding horizon control for multiple unmanned air vehicles formation flight based on chaotic particle swarm optimisation," *IET Control Theory Appl.*, vol. 4, no. 11, pp. 2565–2578, Nov. 2010.
- [18] Z. Qi, Q. Shi, and H. Zhang, "Tuning of digital PID controllers using particle swarm optimization algorithm for a CAN-based DC motor subject to stochastic delays," *IEEE Trans. Ind. Electron.*, vol. 67, no. 7, pp. 5637–5646, Jul. 2020.
- [19] K. D. Sharma, A. Chatterjee, and A. Rakshit, "A PSO–Lyapunov hybrid stable adaptive fuzzy tracking control approach for vision-based robot navigation," *IEEE Trans. Instrum. Meas.*, vol. 61, no. 7, pp. 1908–1914, Jul. 2012.
- [20] N. D. Zoric, A. M. Simonović, Z. S. Mitrović, and S. N. Stupar, "Optimal vibration control of smart composite beams with optimal size and location of piezoelectric sensing and actuation," *J. Intell. Mater. Syst. Struct.*, vol. 24, no. 4, pp. 499–526, Mar. 2013.
- [21] *Active Suspension—User Manual*, Quanser, Markham, ON, Canada, 2013.
- [22] M. Dorigo, "Optimization, learning and natural algorithms," Ph.D. dissertation, Dept. Electron., Politecnico di Milano, Milan, Italy, 1992.
- [23] M. Dorigo and T. Stützle, *Ant Colony Optimization*, New York, NY, USA: MIT Press, 2004.
- [24] M. Dorigo and L. M. Gambardella, "Ant colonies for the travelling salesman problem," *Biosystems*, vol. 43, no. 2, pp. 73–81, 1997.
- [25] P. Pechac, "Electromagnetic wave propagation modeling using the ant colony optimization algorithm," *Radio Eng.*, vol. 11, pp. 1–6, 2002.
- [26] Q. Wu, J. Zhang, and X. Xu, "Variability of ant colony algorithm," *Comput. Res. Develop.*, vol. 36, no. 10, pp. 1–8, 1999.
- [27] M. Q. Nguyen, M. Canale, O. Sename, and L. Dugard, "A model predictive control approach for semi-active suspension control problem of a full car," in *Proc. IEEE 55th Conf. Decis. Control (CDC)*, Las Vegas, NV, USA, Dec. 2016, pp. 721–726, doi: [10.1109/CDC.2016.7798353](https://doi.org/10.1109/CDC.2016.7798353).



**SAIBAL MANNA** received the M.Tech. degree in control & automation from VIT, Vellore, India, in 2019. He is currently pursuing the Ph.D. degree with the Department of Electrical Engineering, NIT Jamshedpur, India. His research interests include adaptive control, optimal control, renewable energy, active suspension systems, and modern control systems.



**GEETHA MANI** received the B.E. degree in electronic and instrumentation engineering from Madurai Kamaraj University, the M.E. degree in instrumentation engineering from MIT Campus, Anna University, India, and the Doctor of Philosophy degree in the field of advanced process control from Anna University, Chennai. She has been teaching for 14 years at reputed institutions. Presently, she is an Associate Professor with the School of Electrical Engineering, Vellore Institute of Technology, Vellore, India. She was a recipient of the IEI Young Engineers Award to recognize her contribution in the field of electrical engineering, in 2016, from the Institution of Engineers, India. She authored and published several research articles in peer-reviewed international journals and book chapters. Her research interests include process control, soft sensing, industrial automation, and the Internet of Things.



**SUSHIL GHILDYAL** is currently pursuing the Ph.D. degree with the Department of Computer Science and Engineering, IIT Ropar. He has been a Researcher working in machine learning algorithms. His current research interest includes applying neural networks in agricultural sectors. He has worked on different robotics projects in his master's.



**VIVEKANANDA GANJI** received the Ph.D. degree in electrical and electronics engineering from Acharya Nagarjuna University (ANU), India. He is currently with the Department of Electrical and Computer Engineering, Debre Tabor University, Ethiopia. His current research interests include power systems and electric vehicle (EV).



**ALBERT ALEXANDER STONIER** (Senior Member, IEEE) was born in Tamil Nadu, India. He was a Postdoctoral Research Fellow with Northeastern University, Boston, MA, USA. He is currently working as an Associate Professor with the Department of Electrical and Electronics Engineering, Kongu Engineering College, India. He is also the Vice President of the Energy Conservation Society, India. His research interests include neural networks and fuzzy logic control for power

converters, solar energy conversion systems, and smart grid. He has received 25 awards from national and international societies; a few to say are recipient of the Teaching Innovator Award (National Level) from MHRD, Government of India, in 2019, the Premium Award for Best Paper in IET Renewable Power Generation, in 2017, and the Best Researcher Award from IEEE Madras Section and IET, in 2021.



**GENO PETER** received the Doctor of Philosophy (Ph.D.) degree in electrical engineering from Anna University, India. He started his career as a Test Engineer with General Electricals (Transformer Manufacturing Company), India, subsequently worked with Emirates Transformer & Switchgear, Dubai, as a Test Engineer and then with Al-Ahleia Switchgear Company, Kuwait, as a Quality Assurance Engineer. He is currently working with the School of Electrical and Technology,

University of Technology Sarawak, Malaysia. He is a trained person to work on HAEFELY, Impulse Test System, Switzerland, and a trained person to work on Morgan Schaffer, Dissolved Gas Analyzer Test System, Canada. He has published his research findings in 41 international/national journals. He has presented his research findings in 17 international conferences. He is the author of the book title "A Typical Switchgear Assembly." He is a Chartered Engineer and a Professional Engineer of the Institution of Engineers (India). His research interests include transformers, power electronics, power systems, switchgears, and smart grid & electric vehicle (EV) technology.



**SRINIVASAN MURUGESAN** was born in Tamil Nadu, India, in 1987. He received the B.E. degree in electrical engineering from the Erode Sengunthar Engineering College, Erode, India, the M.E. degree in high voltage engineering from the National Engineering College, India, and the Ph.D. degree from Anna University, Chennai. He is currently working as an Assistant Professor with the Kongu Engineering College. He has acquired various funds from DST, DRDO, DBT, and ISRO for

power packed seminars, workshops, and research projects. In his efforts, he has set up High Voltage Liquid Dielectric Testing Laboratory with the financial grant from DST-FIST. He was a recipient of SERB TARE Research Fellowship and pursuing research at IIT Madras. His research interests include alternative insulating fluids, eco-friendly fire-resistant fluids, insulation engineering, and power systems.

...